LETTERS

mTOR controls mitochondrial oxidative function through a YY1–PGC-1α transcriptional complex

John T. Cunningham[1,2], Joseph T. Rodgers[1], Daniel H. Arlow[3], Francisca Vazquez[1], Vamsi K. Mootha[3] & Pere Puigserver[1,2]

Transcriptional complexes that contain peroxisome-proliferator-activated receptor coactivator (PGC)-1α control mitochondrial oxidative function to maintain energy homeostasis in response to nutrient and hormonal signals[1,2]. An important component in the energy and nutrient pathways is mammalian target of rapamycin (mTOR), a kinase that regulates cell growth, size and survival[3–5]. However, it is unknown whether and how mTOR controls mitochondrial oxidative activities. Here we show that mTOR is necessary for the maintenance of mitochondrial oxidative function. In skeletal muscle tissues and cells, the mTOR inhibitor rapamycin decreased the gene expression of the mitochondrial transcriptional regulators PGC-1α, oestrogen-related receptor α and nuclear respiratory factors, resulting in a decrease in mitochondrial gene expression and oxygen consumption. Using computational genomics, we identified the transcription factor yin-yang 1 (YY1) as a common target of mTOR and PGC-1α. Knockdown of YY1 caused a significant decrease in mitochondrial gene expression and in respiration, and YY1 was required for rapamycin-dependent repression of those genes. Moreover, mTOR and raptor interacted with YY1, and inhibition of mTOR resulted in a failure of YY1 to interact with and be coactivated by PGC-1α. We have therefore identified a mechanism by which a nutrient sensor (mTOR) balances energy metabolism by means of the transcriptional control of mitochondrial oxidative function. These results have important implications for our understanding of how these pathways might be altered in metabolic diseases and cancer.

Growth factors including insulin induce phosphatidylinositol-3-OH kinase, which activates protein kinase B/Akt, leading to phosphorylation of the tuberous sclerosis (TSC)1–TSC2 complex. This in turn releases Rheb from its inhibition, which then activates the mTOR kinase[4]. mTOR also responds to nutrients through a less well characterized mechanism through Rheb and the class III PI(3)K Vps34 (refs 6–8). mTOR controls the transcription of many genes[9] and positively regulates mitochondrial activity[10]; however, the mechanisms mediating this response remain unknown. PGC-1α controls mitochondrial function through interaction with transcription factors such as oestrogen-related receptor α (ERR-α) and nuclear respiratory factors (NRFs)[11]. Decreases in PGC-1α and PGC-1β and downregulation of oxidative phosphorylation target genes in skeletal muscle have been associated with insulin resistance and type 2 diabetes[12,13].

Taking these results together, we proposed that mTOR might influence nutrient oxidative rates to maintain energy levels in mammalian cells by controlling mitochondrial transcriptional regulators. Figure 1a and Supplementary Fig. 1 show that treatment of C2C12

myotubes with rapamycin (a specific mTOR inhibitor) decreased the messenger RNAs encoding PGC-1α, ERR-α, NRF-1 and Gabpa/b. Mitochondrial gene targets of PGC-1α involved in oxidative phosphorylation, the tricarboxylic acid cycle and uncoupling respiration were also downregulated by rapamycin (Fig. 1b and Supplementary Fig. 1). These effects on gene expression translated into a 32% decrease in mitochondrial DNA content (Fig. 1d) and a 12% decrease in oxygen consumption by rapamycin (Fig. 1e). Similar results were also observed in primary skeletal muscle cells treated with rapamycin (Supplementary Fig. 2). To demonstrate further that mTOR controls mitochondrial genes, we used $TSC2^{-/-}$ cells, in which mTOR is constitutively active[14]. As shown in Fig. 1a–c and Supplementary Fig. 1, $TSC2^{-/-}$ cells showed an elevated expression of mitochondrial genes that were downregulated by rapamycin. Moreover, knockdown of components of the mTORC1 complex, mTOR and raptor, but not S6K1, resulted in decreased expression of mitochondrial genes, and the cells became insensitive to rapamycin (Fig. 1f, 1g, and Supplementary Fig. 3). Mitochondrial DNA content (Fig. 1d) and oxygen consumption (Fig. 1e) followed the same pattern. Next, we investigated whether the effects of rapamycin were also observed in mice. Skeletal muscle from mice treated with rapamycin showed a decrease in mitochondrial gene expression and oxygen consumption (Fig. 1h, i). Mice treated with rapamycin developed symptoms of diabetes, with hyperglycaemia, glucose intolerance, higher levels of free fatty acids in skeletal muscle, hypertriglyceraemia and hyper-cholesterolaemia (Supplementary Fig. 4). Further analysis of the metabolic effects of mTOR in cells treated with rapamycin revealed a decrease in lactate production. Despite lower rates of oxygen consumption and glycolysis, ATP levels were preserved (Supplementary Fig. 5). Because rapamycin can lead to changes in Akt activity through feedback mechanisms[15,16], we determined whether Akt mediated the effects on mitochondrial function. Whereas mitochondrial gene expression and oxygen consumption were decreased after 12 hours of treatment with rapamycin, phospho-Akt was either increased in $TSC2^{-/-}$ cells or unchanged in C2C12 cells. Furthermore, whereas rapamycin decreased expression of the genes encoding PGC-1α and cytochrome c, an Akt inhibitor did not (Supplementary Fig. 6). Taken together, these results support the finding that mTOR positively controls mitochondrial gene expression and oxygen consumption in an Akt-independent manner.

To systematically identify the transcription factors downstream of mTOR that are specifically involved in regulating mitochondrial function, we used a computational genomics approach. We performed microarray analysis of $TSC2^{-/-}$ cells treated with rapamycin (Supplementary Table 1; rapamycin versus vehicle). Using SAM[17], we identified 1,907 differentially expressed genes at an estimated false

[1]Dana-Farber Cancer Institute and Department of Cell Biology, Harvard Medical School, Boston, Massachusetts 02115, USA. [2]Department of Cell Biology, Johns Hopkins University School of Medicine, Baltimore, Maryland 21205, USA. [3]Departments of Systems Biology and Medicine, Massachusetts General Hospital, Harvard Medical School, Boston, Massachusetts 02114, USA and Broad Institute of Massachusetts Institute of Technology and Harvard, Cambridge, Massachusetts 02139, USA.

discovery rate (FDR) of 6.3%. Roughly twice as many transcripts were downregulated as were upregulated, and the downregulated transcripts were highly enriched (12.9% of downregulated transcripts versus 3.7% overall, $P < 8 \times 10^{-45}$) for transcripts predicted to encode mitochondrial proteins[18]. Because PGC-1α is known to regulate the expression of many mitochondrial genes, we also profiled $TSC2^{-/-}$ cells overexpressing $PGC-1\alpha$ (Supplementary Table 2). As seen in Fig. 2a, many of the mitochondrial genes induced by PGC-1α are suppressed by rapamycin; whereas 27% of all genes are in the upper left quadrant, 50% of mitochondrial genes[18] are found in the same quadrant ($\chi^2 = 463$, $P < 9 \times 10^{-103}$). Together, these microarray analyses demonstrate that treatment with rapamycin suppresses the expression of many mitochondrial genes that are induced by PGC-1α. We next used motifADE[11] to identify *cis*-regulatory elements that might mediate the transcriptional response to rapamycin. Among all possible hexamer, heptamer and octamer motifs, the hexamer ATGGCG was the highest scoring element (adjusted $P < 6 \times 10^{-9}$) (Fig. 2b). This hexameric sequence is known to be bound by the transcription factor YY1 (ref. 19). The identified YY1 motif was enriched upstream of predicted mitochondrial genes[18] (24% versus 15%, $P < 3 \times 10^{-11}$) and highly enriched upstream of oxidative phosphorylation genes (36% versus 15%, $P < 5 \times 10^{-5}$).

Because PGC-1α upregulates mitochondrial genes and rapamycin downregulates a large set of these genes (Fig. 2a), we used motifADE to test whether genes with the YY1-binding site are induced during PGC-1α-mediated mitochondrial biogenesis. We found that the hexameric motif was highly significant in the $TSC2^{-/-}$ cells ($P < 2 \times 10^{-7}$) and in C2C12 myotubes ($P < 4 \times 10^{-6}$) overexpressing $PGC-1\alpha$.
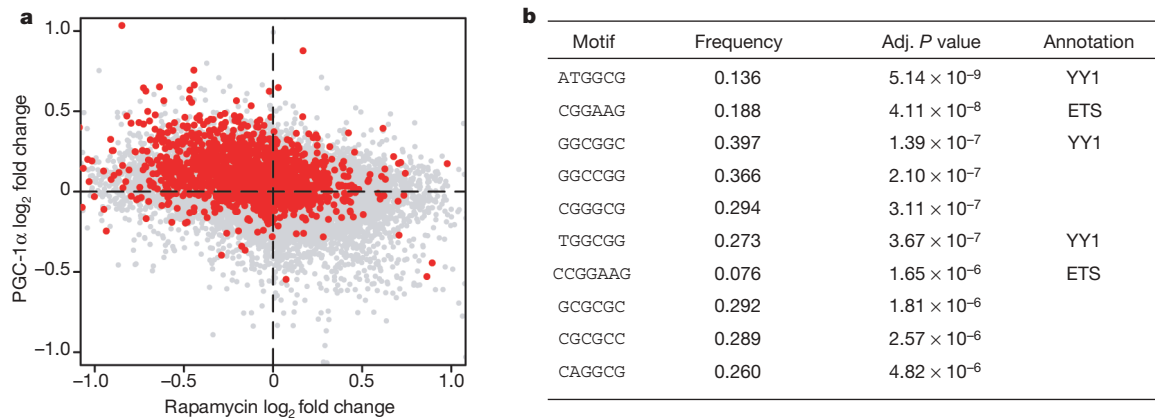
YY1-binding motifs were highly enriched in mitochondrial genes regulated by rapamycin and PGC-1α, suggesting that YY1 might control their expression. Figure 3 shows that knockdown of YY1 decreased the expression of $PGC-1\alpha$ and $PGC-1\beta$, mitochondrial genes, mitochondrial DNA and oxygen consumption. Conversely, ectopic expression of YY1 increased the expression of mitochondrial genes (Fig. 3e). Rapamycin-dependent downregulation of those genes was largely abolished by knockdown of YY1. This indicates that YY1 is required for conferring rapamycin-dependent downregulation.

To gain insights into the mechanisms by which mTOR controls the YY1–PGC-1α function, we performed chromatin immunoprecipitation (ChIP) analysis and found that YY1 is recruited to promoter regions of the genes encoding PGC-1α and cytochrome *c* (Fig. 4a). Moreover, overexpression of YY1 increased, but knockdown of YY1 decreased, the activity of both promoters (Fig. 4b). Because PGC-1α
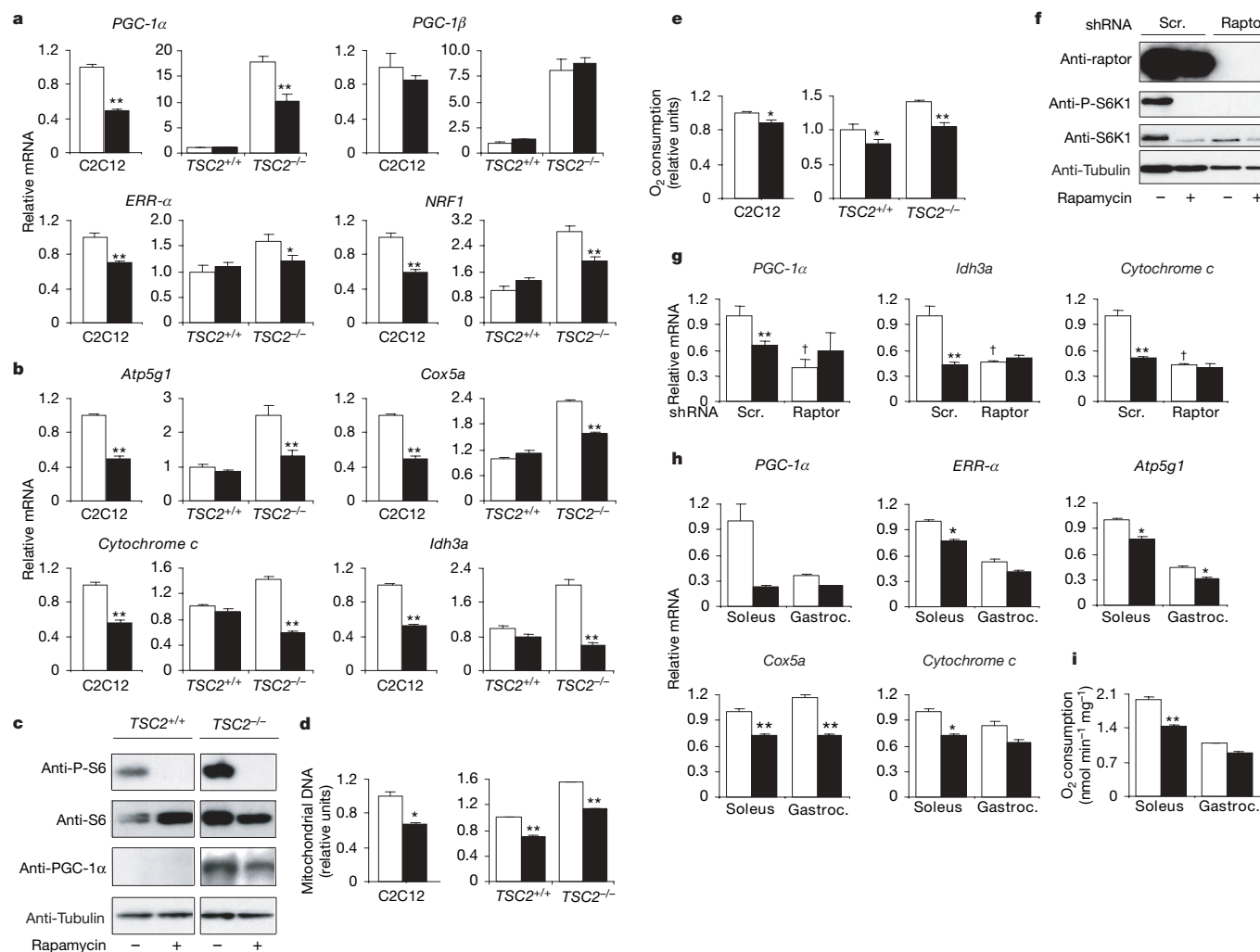
Figure 1 | mTOR controls mitochondrial gene expression and oxygen consumption. a, b, Transcriptional regulators (**a**) and mitochondrial genes (**b**) are regulated by mTOR. Open columns, vehicle; filled columns, rapamycin treatment. **c–e,** RNA and protein (**c**), mitochondrial DNA (**d**) and oxygen consumption (**e**) are decreased by rapamycin. **f, g,** Raptor knockdown decreases PGC-1α and mitochondrial genes. Lentiviral shRNAs were used to infect $TSC2^{-/-}$ cells. Scr., scrambled. **f,** Western blot analysis of

indicated proteins. **g,** Quantitative real-time PCR analysis of indicated genes. **h, i,** Rapamycin decreases mitochondrial genes (**h**) and oxygen consumption (**i**) in mouse skeletal muscle. Gastroc., gastrocnemius. Measurements are described in Methods. Error bars represent s.e.m.; $n = 6$; asterisk, $P < 0.05$; two asterisks, $P < 0.01$ for vehicle versus rapamycin treatment; dagger, $P < 0.05$ scrambled versus raptor shRNA.

Motif	Frequency	Adj. P value	Annotation
ATGGCG	0.136	5.14×10^{-9}	YY1
CGGAAG	0.188	4.11×10^{-8}	ETS
GGCGGC	0.397	1.39×10^{-7}	YY1
GGCCGG	0.366	2.10×10^{-7}	
CGGGCG	0.294	3.11×10^{-7}	
TGGCGG	0.273	3.67×10^{-7}	YY1
CCGGAAG	0.076	1.65×10^{-6}	ETS
GCGCGC	0.292	1.81×10^{-6}	
CGCGCC	0.289	2.57×10^{-6}	
CAGGCG	0.260	4.82×10^{-6}	

Figure 2 | Genomic analysis reveals that mitochondrial genes are regulated by PGC-1α and mTOR pathways by means of the transcription factor YY1. a, Relationship between the change in expression of all genes in $TSC2^{-/-}$ cells treated with rapamycin (x axis) and overexpressing PGC-1α (y axis). Mitochondrial genes[18] are shown in red; 50% of mitochondrial genes are found in the upper left quadrant, whereas only 27% of all genes are found in the quadrant ($P < 9 \times 10^{-103}$). **b**, MotifADE output showing the top ten most significant motifs for rapamycin versus vehicle in $TSC2^{-/-}$ cells. The YY1-binding site is the highest-scoring motif in cells treated with rapamycin. Adj., adjusted.

regulates both genes[11], we analysed whether YY1 was coactivated by PGC-1α. As shown in Fig. 4c, PGC-1α increased the transcriptional activity of GAL4-YY1. PGC-1α coactivation of YY1, but not of ERR-α, was repressed by rapamycin. These results indicate that YY1 binds directly to mitochondrial gene promoters and that PGC-1α functions as a transcriptional coactivator for YY1 in an mTOR-dependent manner. To test how mTOR might control YY1, we performed immunoprecipitation assays. As shown in Fig. 4d, mTOR is present in the YY1 protein complex. This interaction is direct and requires both the YY1 amino and carboxy termini (Supplementary Fig. 7b). Raptor (a component of mTORC1), but not rictor (a component of mTORC2) also interacted with YY1 and was bound to promoters of the genes encoding PGC-1α and cytochrome c (Fig. 4a, e). In addition, mapping studies indicated that raptor binds to the YY1 region that lies between amino-acid residues 203 and 235, which has been shown to be necessary for co-repressor recruitment (Supplementary Fig. 7e)[20]. In binding assays in vitro, glutathione S-transferase (GST)–YY1 interacted strongly with full-length PGC-1α through the C-terminal domain. In addition, PGC-1α interacted with YY1 primarily through the third C-terminal zinc finger (Supplementary Fig. 7h). Finally, the fact that coactivation of YY1 by PGC-1α was decreased by rapamycin while YY1 remained bound to the
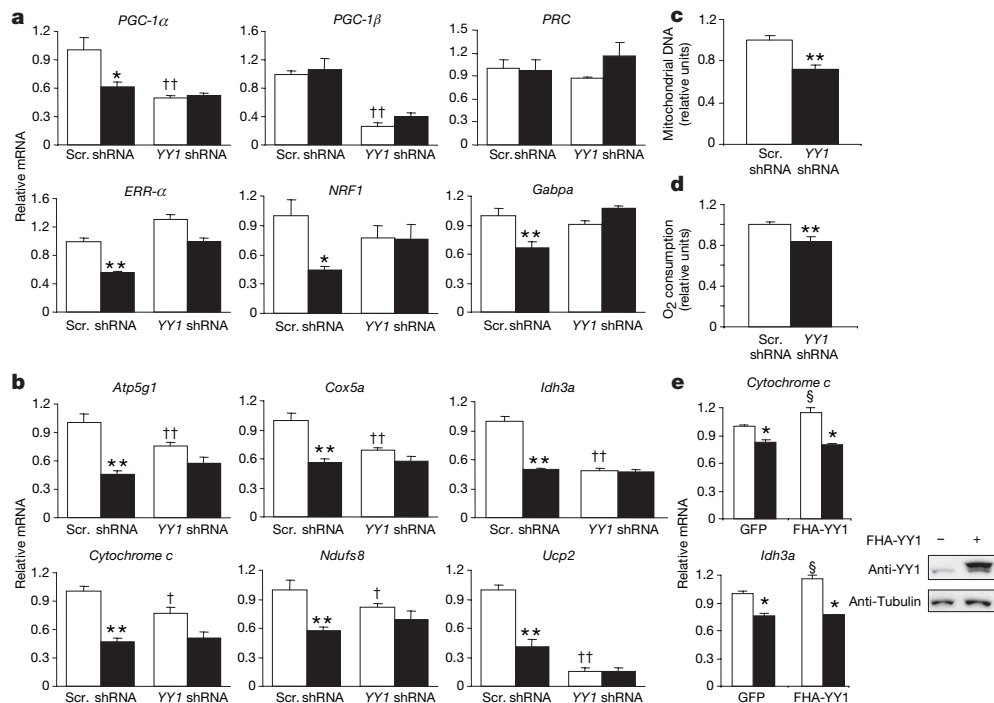
Figure 3 | YY1 regulates mitochondrial gene expression and oxygen consumption. a, PGC-1α and PGC-1β are controlled by YY1. C2C12 myotubes were infected with adenoviruses encoding scrambled (scr.) or *YY1* shRNA. RNA was quantified as described in Methods. Open columns, vehicle; filled columns, rapamycin treatment. PRC, PGC-1-related coactivator. **b–d**, Mitochondrial gene expression (**b**), mitochondrial DNA (**c**) and oxygen consumption (**d**) are decreased by *YY1* shRNA. In **b**, open columns, vehicle; filled columns, rapamycin treatment. **e**, Ectopic expression of *YY1* increased mitochondrial genes. HEK-293 cells were infected with lentiviruses encoding YY1 as described in Methods. FHA, Flag–HA epitope tag. Open columns, vehicle; filled columns, rapamycin treatment. Error bars represent s.e.m.; $n = 6$; asterisk, $P < 0.05$; two asterisks, $P < 0.01$ for vehicle versus rapamycin; dagger, $P < 0.05$; two daggers, $P < 0.01$ for scrambled versus *YY1* shRNA; section sign, $P < 0.05$ for GFP versus FHA-YY1.
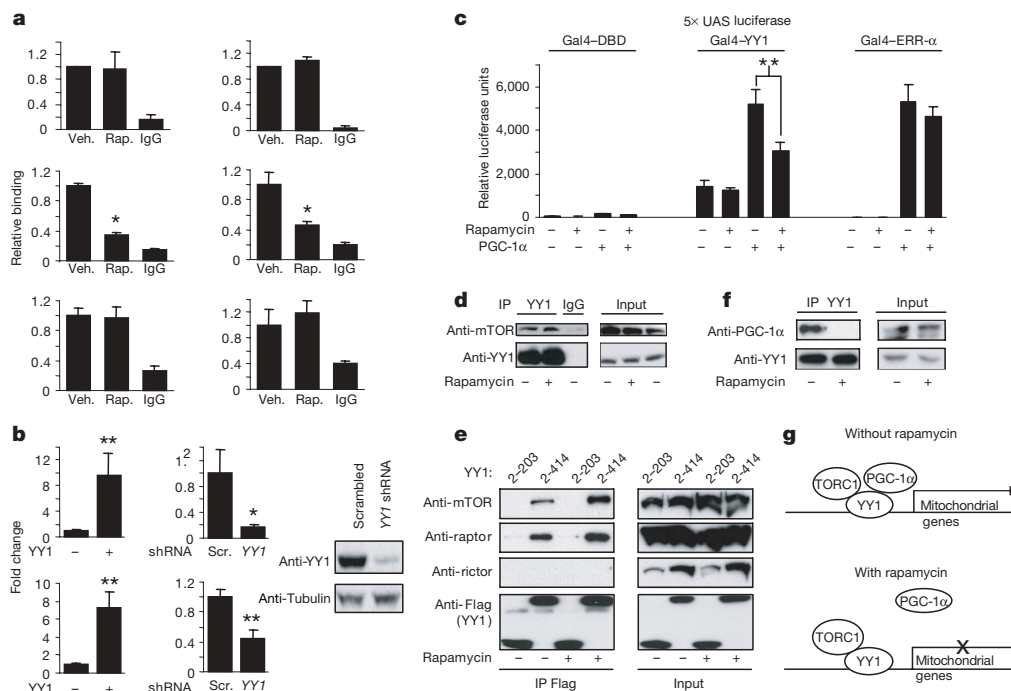
Figure 4 | Rapamycin-dependent coactivation and interaction between PGC-1α, YY1 and mTORC1. a, YY1, PGC-1α and raptor bind the promoters of the genes encoding PGC-1α (left panels) and cytochrome *c* (right panels). ChIP analysis with YY1 (top row), Flag–HA–PGC-1α (middle row) and raptor (bottom row) was performed on $TSC2^{-/-}$ cells. Bars represent s.e.m.; *n* = 6. **b,** YY1 activates the promoters of the genes encoding cytochrome *c* (top graphs) and PGC-1α (bottom graphs). Luciferase reporter assay.

c, YY1–PGC-1α transcriptional activity is repressed by rapamycin. Error bars represent s.e.m.; *n* = 8; asterisk, *P* < 0.05; two asterisks, *P* < 0.01 for vehicle versus rapamycin treatment in **c**, and for versus vector controls in **b**. **d, e,** mTOR (**d**) and raptor (**e**) interact with YY1. IP, immunoprecipitation. **f,** Rapamycin-dependent interaction between YY1 and PGC-1α. YY1 immunoprecipitates were analysed by western blot. **g,** Model of how mTOR controls mitochondrial respiration.

promoters, and that mTOR and raptor interacted with YY1 independently of rapamycin, prompted us to test whether the interaction between YY1 and PGC-1α was the key regulated step that controlled YY1-dependent mitochondrial gene transcription in response to mTOR activity. Figure 4f and Supplementary Fig. 7j show that PGC-1α and YY1 interacted in cells; more significantly, the interaction between these two proteins was disrupted by rapamycin. ChIP analysis showed that PGC-1α is bound to promoters of the genes encoding cytochrome *c* and PGC-1α; however, rapamycin prevented this recruitment (Fig. 4a). These results indicate that mTOR regulates the transcriptional function of YY1–PGC-1α by directly altering their physical interaction.

Transcription factors such as ERR-α and Gabpa/b are important for PGC-1α-induced mitochondrial biogenesis[11,21]; however, mTOR did not directly regulate the transcriptional activity of PGC-1α on these factors. Instead, mTOR controlled mitochondrial gene expression through the direct modulation of YY1–PGC-1α activity. This regulation would allow the cell to connect nutrient pathways to activate mitochondrial function and ensure energy supply for cellular activities. PGC-1α and oxidative phosphorylation genes are modestly downregulated in skeletal muscle of humans with type 2 diabetes[12,13]. Our motif analysis also identified the YY1 motif as being significantly associated with this pattern of mitochondrial gene expression. In fact, the YY1 motif is also significantly (*P* < 0.05) associated with differential expression between diabetic and control patients[12]. However, it is not clear how mTOR is regulated in skeletal muscle in type 2 diabetes and insulin resistance. We show that mice treated with rapamcyin developed several symptoms of diabetes, which is consistent with diminished oxidative function in skeletal muscle. Treatment with rapamycin in humans receiving organ transplants and in rodents has been associated with increased levels of blood triacylglycerols and cholesterol, which might contribute to insulin resistance[22,23]. Our model (Fig. 4g) predicts that a decrease in mTOR activity would inhibit YY1–PGC-1α function, resulting in a decreased expression of mitochondrial genes that might be linked to increased circulating and intracellular lipids. Finally, the fact that the YY1–PGC-1α interaction can be directly modulated by mTOR activity opens new possibilities for potential pharmacological intervention to increase mitochondrial activity in metabolic diseases in which it is compromised.

METHODS SUMMARY

Experiments on mice. Male Balb/c mice 10 weeks old were daily injected intraperitoneally with 2.5 mg kg^{-1} rapamycin or vehicle. Mice were sacrificed after 11 days of injection and soleus and gastrocnemius muscles were dissected. Oxygen consumption was measured from saponin-permeabilized muscle slices using 5 mM glutamate and 2 mM malate as substrates, as described, with a Rank Brothers oxygen electrode[24,25].

Molecular biology. Cells were cultured in DMEM containing 10% cosmic calf serum. C2C12 myoblasts were differentiated in DMEM with 2% horse serum. YY1 short hairpin RNA (shRNA) was cloned into pSUPER by using the sequence 5′-GGGAGCAGAAGCAGGTGCAGAT-3′. Other expression and shRNA plasmids have been described previously or were generated by PCR cloning of described constructs (see Methods). RNA was isolated with Trizol, reverse transcribed using Superscript II Reverse Transcriptase with oligo(dT) primers and analysed by quantitative real-time (qRT)–PCR by SYBR green fluorescence. Mitochondrial DNA was quantified by determining the ratio of mitochondrial cyclo-oxygenase (Cox)2 to nuclear intron of β-globin by qRT–PCR of isolated DNA. ChIP was performed by using the Upstate protocol with the indicated antibodies. Luciferase assays were performed on lysates after transfection of cells with the indicated plasmids by using Polyfect reagent.

Microarray and *cis*-regulatory motif analysis. Expression profiles of $TSC2^{-/-}$ cells were obtained with Affymetrix MOE430v2 GeneChips. Expression summary values were calculated by using RMA[26] with default settings in one batch for the rapamycin/vehicle-treated cells and separately for the PGC-1α/green fluorescent protein (GFP)-transduced cells. A modified version of motifADE[11] was used to identify *cis* elements associated with differential expression between treatment groups. Promoter regions consisting of 2 kilobases of genomic sequence centred on the transcription start site were compiled, and a gene was recorded as having a particular motif only if both mouse and human promoters contained the motif, although the position need not be conserved. A Bonferroni

correction was applied when testing all *k*-mer motifs. The hypergeometric distribution was used to test whether the YY1 motif was enriched upstream of nuclear-encoded oxidative phosphorylation and mitochondrial genes[18].

1. Finck, B. N. & Kelly, D. P. PGC-1 coactivators: inducible regulators of energy metabolism in health and disease. *J. Clin. Invest.* **116**, 615–622 (2006).
2. Lin, J., Handschin, C. & Spiegelman, B. M. Metabolic control through the PGC-1 family of transcription coactivators. *Cell Metab.* **1**, 361–370 (2005).
3. Wullschleger, S., Loewith, R. & Hall, M. N. TOR signaling in growth and metabolism. *Cell* **124**, 471–484 (2006).
4. Dann, S. G. & Thomas, G. The amino acid sensitive TOR pathway from yeast to mammals. *FEBS Lett.* **580**, 2821–2829 (2006).
5. Sarbassov, D. D., Ali, S. M. & Sabatini, D. M. Growing roles for the mTOR pathway. *Curr. Opin. Cell Biol.* **17**, 596–603 (2005).
6. Inoki, K., Li, Y., Xu, T. & Guan, K. L. Rheb GTPase is a direct target of TSC2 GAP activity and regulates mTOR signaling. *Genes Dev.* **17**, 1829–1834 (2003).
7. Long, X., Lin, Y., Ortiz-Vega, S., Yonezawa, K. & Avruch, J. Rheb binds and regulates the mTOR kinase. *Curr. Biol.* **15**, 702–713 (2005).
8. Nobukini, T. *et al.* Amino acids mediate mTOR/raptor signaling through activation of class 3 phosphatidylinositol 3OH-kinase. *Proc. Natl Acad. Sci. USA* **102**, 14238–14243 (2005).
9. Peng, T., Golub, T. R. & Sabatini, D. M. The immunosuppressant rapamycin mimics a starvation-like signal distinct from amino acid and glucose deprivation. *Mol. Cell. Biol.* **22**, 5575–5584 (2002).
10. Schieke, S. M. *et al.* The mammalian target of rapamycin (mTOR) pathway regulates mitochondrial oxygen consumption and oxidative capacity. *J. Biol. Chem.* **281**, 27643–27652 (2006).
11. Mootha, V. K. *et al.* Errα and Gabpa/b specify PGC-1α-dependent oxidative phosphorylation gene expression that is altered in diabetic muscle. *Proc. Natl Acad. Sci. USA* **101**, 6570–6575 (2004).
12. Mootha, V. K. *et al.* PGC-1α-responsive genes involved in oxidative phosphorylation are coordinately downregulated in human diabetes. *Nature Genet.* **34**, 267–273 (2003).
13. Patti, M. E. *et al.* Coordinated reduction of genes of oxidative metabolism in humans with insulin resistance and diabetes: Potential role of PGC1 and NRF1. *Proc. Natl Acad. Sci. USA* **100**, 8466–8471 (2003).
14. Zhang, H. *et al.* Loss of Tsc1/Tsc2 activates mTOR and disrupts PI3K–Akt signaling through downregulation of PDGFR. *J. Clin. Invest.* **112**, 1223–1233 (2003).
15. Shah, O. J., Wang, Z. & Hunter, T. Inappropriate activation of the TSC/Rheb/mTOR/S6K cassette induces IRS1/2 depletion, insulin resistance, and cell survival deficiencies. *Curr. Biol.* **14**, 1650–1656 (2004).
16. Sarbassov, D. D. *et al.* Prolonged rapamycin treatment inhibits mTORC2 assembly and Akt/PKB. *Mol. Cell* **22**, 159–168 (2006).
17. Tusher, V. G., Tibshirani, R. & Chu, G. Significance analysis of microarrays applied to the ionizing radiation response. *Proc. Natl Acad. Sci. USA* **98**, 5116–5121 (2001).
18. Calvo, S. *et al.* Systematic identification of human mitochondrial disease genes through integrative genomics. *Nature Genet.* **38**, 576–582 (2006).
19. Yant, S. R. *et al.* High affinity YY1 binding motifs: identification of two core types (ACAT and CCAT) and distribution of potential binding sites within the human beta globin cluster. *Nucleic Acids Res.* **23**, 4353–4362 (1995).
20. Wilkinson, F. H., Park, K. & Atchison, M. L. Polycomb recruitment to DNA *in vivo* by the YY1 REPO domain. *Proc. Natl Acad. Sci. USA* **103**, 19296–19301 (2006).
21. Schreiber, S. N. *et al.* The estrogen-related receptor α (ERRα) functions in PPARγ coactivator 1α (PGC-1α)-induced mitochondrial biogenesis. *Proc. Natl Acad. Sci. USA* **101**, 6472–6477 (2004).
22. Ribes, D., Kamar, N., Esposito, L. & Rostaing, L. Combined use of tacrolimus and sirolimus in *de novo* renal transplant patients: current data. *Transplant. Proc.* **37**, 2813–2816 (2005).
23. Morrisett, J. D. *et al.* Effects of sirolimus on plasma lipids, lipoprotein levels, and fatty acid metabolism in renal transplant patients. *J. Lipid Res.* **43**, 1170–1180 (2002).
24. Leone, T. C. *et al.* PGC-1α deficiency causes multi-system energy metabolic derangements: muscle dysfunction, abnormal weight control and hepatic steatosis. *PLoS Biol.* **3**, e101 (2005).
25. Saks, V. A. *et al.* Permeabilized cell and skinned fiber techniques in studies of mitochondrial function *in vivo*. *Mol. Cell. Biochem.* **184**, 81–100 (1998).
26. Irizarry, R. A. *et al.* Summaries of Affymetrix GeneChip probe level data. *Nucleic Acids Res.* **31**, e15 (2003).

METHODS

Constructs and reagents. Adenoviruses were constructed using the pAdEASY system (Stratagene). The cytochrome *c* and 2-kilobase PGC-1α pGL3 luciferase reporter plasmids have been described previously[11,27]. Gal4–ERR-α and Gal4–YY1 constructs were made by cloning full-length complementary DNAs into pCMX-R *Eco*RI/*Bam*HI and *Bam*HI/*Nhe*I sites, respectively. Flag–haemagglutinin (HA)–YY1 was cloned into VVCW/BE for lentiviral expression by using *Eco*RI/*Not*I sites. Antibodies used were: phospho-S6K1 (catalogue no. 9205; Cell Signaling), S6K1 (catalogue no. 9202; Cell Signaling), phospho-S6 (catalogue no. 2211; Cell Signaling), S6 (catalogue no. 2212; Cell Signaling), tubulin (catalogue no. 05-661; Upstate), mTOR (catalogue no. 2972; Cell Signaling), raptor (catalogue no. 4978; Cell Signaling) and rictor (catalogue no. 2140; Cell Signaling).

Cell culture and treatments. C2C12 cells were differentiated using DMEM containing 2% horse serum for 72 h before treatments or infections. Infected C2C12 cells were analysed or treated with vehicle or rapamycin (14 h at 20 nM unless otherwise indicated) 72 h after infection.

ChIP. Chromatin:protein complexes were prepared from cells using the Upstate protocol. For Raptor and Flag–HA–PGC-1α experiments, 1.5 mM DSP[28] was used to crosslink protein:protein/DNA complexes in addition to 1% formaldehyde. DNA was sheared to 200–800-base-pair fragments and immunoprecipitated with rabbit anti-YY1 antibody (catalogue no. sc-281; Santa Cruz), HA-affinity matrix (Roche) or anti-raptor antibodies (catalogue nos 2280 and 4978; Cell Signaling). Primer sequences are provided in Supplementary Information. Ratios of input DNA to bound DNA were calculated and data were normalized to vehicle-treated samples.

Mitochondrial DNA quantification. Cells were treated with dimethylsulphoxide or 20 nM rapamycin for 48 h for *TSC2*$^{-/-}$ cells and for 72 h for C2C12 cells. Mitochondrial DNA was quantified by quantitative real-time PCR by measuring the ratio of mitochondrially encoded Cox2 to an intron of the nuclear-encoded β-globin gene. Similar results were obtained with mitochondrial cytochrome *b* and an intron of nuclear glucagon. Primer sequences are provided in Supplementary Information.

Protein interaction analysis. For immunoprecipitation, nuclear extracts were prepared with the Dignam protocol except that nuclei were lysed in buffer containing 20 mM HEPES pH 7.9, 125 mM NaCl, 0.5% Nonidet P40, 1 mM EDTA, protease and phosphatase inhibitors. YY1 protein was immunoprecipitated using anti-YY1 antibody (catalogue no. sc-281; Santa Cruz). YY1 was western blotted using anti-YY1 antibody (catalogue no. sc-7341; Santa Cruz) and anti-PGC-1α antibody (gift from B. Spiegelman). YY1 and mTORC1 immunoprecipitations were performed with the protocol described[29].

Oxygen consumption analysis. Cells were trypsinized, washed in PBS and then resuspended in Dulbecco's phosphate-buffered saline (dPBS) supplemented with 25 mM glucose, 1 mM pyruvate and 2% BSA. The rate of oxygen consumption was measured with a Rank Brothers oxygen electrode. An equal number of cells under each condition were counted and placed in the electrode chamber for measurement. Data are expressed relative to the rate of respiration of control samples.

Transient transfection, luciferase reporter assays and lentivirus infection. Transient transfections were performed in HEK-293 or *TSC2*$^{-/-}$ murine embryonic fibroblasts using Polyfect (Qiagen) at a DNA:Polyfect ratio of 1:2. Cell culture medium was changed after 12 h. Cells were Lysed with Reporter Lysis Buffer (Promega) and luciferase assays were performed. For lentivirus encoding shRNA experiments, we used the same protocol as described in ref. 30; sequences are provided in Supplementary Information.

Gene expression analysis. Total RNA was extracted with Trizol (Invitrogen). cDNA generated by Superscript II enzyme (Invitrogen) with oligo(dT) primer was analysed by qRT−PCR with an iQ SYBR Green Supermix (Bio-Rad). Cell culture data were normalized to β-actin expression and mouse data were normalized to 36B4 expression. Primer sequences are provided in Supplementary Information.

Microarray analysis. *TSC2*$^{-/-}$ murine embryonic fibroblasts were either (1) treated with vehicle or 20 nM rapamycin for 14 h or (2) infected with adenovirus expressing GFP or PGC-1α for 24 h. RNA was isolated with Trizol reagent. Using Affymetrix MOE430 v2 gene chips, biological triplicates of each condition were analysed: vehicle-treated, rapamycin-treated, GFP-infected and PGC-1α-infected. Expression summary values were computed by using RMA[26] in Bioconductor with default settings (background correction version 1.2, quantile normalization) in one batch for the rapamycin/vehicle-treated cells and in another for the PGC-1α/GFP-infected cells.

Cis-regulatory motif analysis. Databases of promoter regions consisting of 2,000 bases centred on the annotated transcription start site (TSS) of all mouse and human RefSeq genes were prepared using the UCSC genome browser and the MM4 and HG16 builds of the mouse and human genomes. Using an orthology mapping from the Jackson Laboratory, 10,503 mouse/human pairs of promoter regions of orthologous genes were compiled. For all sequence analyses, a gene was recorded as having a particular motif in its promoter region only if the mouse and corresponding human promoter regions both contained an instance of the motif, although the position relative to the TSS need not be conserved. The cumulative hypergeometric distribution was used to test whether the identified YY1 motif ATGGCG was significantly enriched upstream of nuclear-encoded mitochondrial genes and upstream of nuclear-encoded genes involved in oxidative phosphorylation. The Maestro predicted mitochondrial genes were used as a comprehensive list of mitochondrial genes[18]. Of the 10,503 mouse/human pairs in the promoter region database, 712 were Maestro genes and 64 were oxidative phosphorylation genes. Using the annotations from Affymetrix, 4,955 mouse/human promoter region pairs were compiled for which the mouse gene was measured by a single probe set on the Mouse 430A chip. These probe sets were ordered by using Welch's *t* statistic as a measure of differential expression between rapamycin and vehicle, and all hexamer, heptamer and octamer DNA sequences were tested for association with differential expression by using motifADE[11]. To correct for multiple testing, a flat Bonferroni correction of 4^k was applied to the nominal *P* values when testing all *k*-mer motifs. MotifADE was also used to test whether the identified YY1 motif ATGGCG was associated with differential expression in several other data sets[12,18]. In each case, all genes were ordered by differential expression by using Welch's *t* statistic. When testing a single motif (instead of, for example, 4^6 motifs) it is unnecessary to apply the Bonferroni correction.

27. Andersson, U. & Scarpulla, R. C. Pgc-1-related coactivator, a novel, serum-inducible coactivator of nuclear respiratory factor 1-dependent transcription in mammalian cells. *Mol. Cell. Biol.* **21**, 3738–3749 (2001).

28. Pierce, S. B. *et al.* Regulation of DAF-2 receptor signaling by human insulin and *ins-1*, a member of the unusually large and diverse *C. elegans* insulin gene family. *Genes Dev.* **15**, 672–686 (2001).

29. Kim, D. H. *et al.* mTOR interacts with raptor to form a nutrient-sensitive complex that signals to the cell growth machinery. *Cell* **110**, 163–175 (2002).

30. Sancak, Y. *et al.* PRAS40 is an insulin-regulated inhibitor of the mTORC1 protein kinase. *Mol. Cell* **25**, 903–915 (2007).